

03

# Physicomathematical model of icing of the rotating sphere in a coaxial supercooled gas-drop flow

© A.V. Kashevarov, A.L. Stasenko

Central Aerohydrodynamic Institute named after N.E. Zhukovsky,  
140180 Zhukovsky, Russia  
e-mail: a.v.kash@yandex.ru

Received June 21, 2023

Revised July 27, 2023

Accepted July 27, 2023

A physico-mathematical model is proposed for assessing the effect of centrifugal force on the characteristic dimensions of needle-shaped ice formed as a result of the collision of a large supercooled drop with a sphere rotating in a coaxial air flow. The mass loss of droplets upon collision with the surface due to splashing is taken into account. The numerical implementation of the model makes it possible to study the effect of surface properties on the icing process and, in particular, to estimate the ice-free surface area due to centrifugal force.

**Keywords:** supercooled large droplets, droplet splashing, centrifugal force, wetting angle, surface tension, droplet detachment.

DOI: 10.61011/TP.2023.10.57447.155-23

## Introduction

The icing of the body in a supercooled air-drop stream is accompanied by a combination of complex physical phenomena. Certified numerical codes have been created to date in many countries to predict the spatio-temporal evolution of ice on the structural elements of an aircraft. Some of these codes, in particular FENSAP-ICE, also consider icing of rotating engine structural elements. At the same time, additional complications arise in the physical and mathematical modeling of icing. Thus, the results of studies in an air-cooling pipe of ice forms on fans with different shapes of central bodies (cone, ellipsoid and cone with ellipsoidal extension) in a supercooled air stream with drops with a small diameter ( $\sim 20 \mu\text{m}$ ) are presented in [1]. It is found, in particular, that rotation leads to the formation of needle-like icicles on a part of the surface of the central body at some distance from its top, and then an ice-free zone arises due to the breakdown of ice under the action of centrifugal forces. Existing codes do not yet allow modeling such ice growths.

Needle-shaped icicles appeared at a slightly negative temperature of the air flow ( $-5^\circ\text{C}$ ) and a sufficiently large mass concentration of liquid water in it (LWC — Liquid Water Content) under conditions of formation of the so-called glaze ice. At the same time, the supercooled drops did not freeze completely when they hit the surface, forming a flowing liquid film. The formation of needle ice is explained in [1] by the separation of the film from the surface under the action of centrifugal forces, followed by freezing. It is reported in [2] that similar needle formations were found on the engine fan cone in the real flight of A321 aircraft in icy rain conditions, i.e. large supercooled drops.

A discrete-drop model of icing of a transverse non-rotating cylinder under such conditions is proposed in [3],

using the results of experimental and theoretical studies of [4,5] collision of a drop with a flat surface. The discrete-drop approach proposed in [3] is modified and applied in this paper to simulate the shape of a frozen large supercooled drop on the surface of a rotating sphere.

## 1. Preliminary considerations

Consider an air flow with a velocity of  $u_\infty$  carrying large supercooled drops with a radius of  $a_d$ , but they collide with the surface of a rotating sphere with a radius of  $R$  unlike the case of [3]. Drops with a diameter of more than  $100 \mu\text{m}$  are considered as „large“ according to international airworthiness standards.

The flow pattern of a drops on a rotating sphere is shown in Fig. 1. Note that the angular velocity of rotation of the sphere  $W$  is depicted in the „fixed“ coordinate system. The rotation of the sphere results in the formation of a flow around the surface of the sphere in the opposite direction indicated by the vector  $\mathbf{V}_w$ . However, the choice of the direction of rotation of the sphere with axisymmetric flow does not affect the result of icing.

In case of a collision the drop splashes and only part of  $m$  of its original mass  $m_0$  remains on the surface. An approximation dependence of the coefficient  $\xi = m/m_0$  on the angle of incidence of  $\alpha$  drops is proposed for a fixed surface in [3], based on the results of [4].

$$\xi = \frac{m}{m_0} = \left[ 1 - \left| \frac{R_s - R_l}{R_s + R_l} \right|^3 \frac{d_0}{d_*} \left( \frac{v_n}{v_*} \right)^{2/3} \left( \frac{\mu_*}{\mu_l} \right)^{1/2} \times \cos^2 \alpha \right] \cos^{1/6} \alpha \geq 0.$$

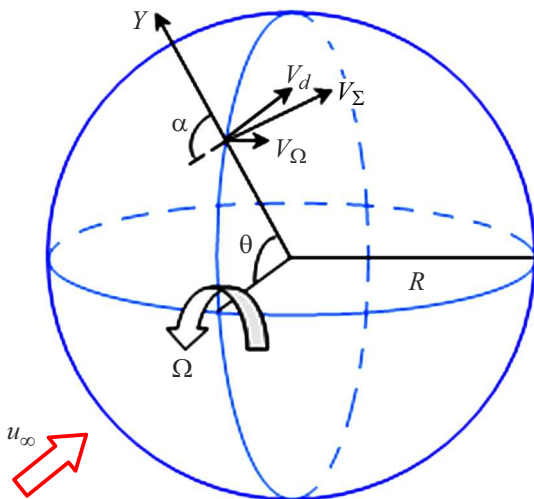


**Figure 1.** Geometry of a rotating sphere. The angular velocity  $\Omega$  is given in the laboratory coordinate system, the components of the drop velocities — in the local non-inertial system.

Here  $R_{s,l} = \rho_{s,l} c_{s,l}$  — wave resistances (impedances) of materials of a streamlined body and drops ( $\rho_{s,l}$  and  $c_{s,l}$  — their densities and sound velocities in them,  $s$  — solid,  $l$  — liquid),  $v_n$  — normal component of the impact velocity,  $\mu_l$  — viscosity of the liquid. The values of the reference parameters:  $d_* = 250 \mu\text{m}$ ,  $v_* = 80 \text{ m/s}$ ,  $\mu_* = 1.75 \cdot 10^{-3} \text{ Pa} \cdot \text{s}$ .

The effect of rotation on the fraction  $\xi$  of the mass remaining on the surface is determined by changing the angle of incidence  $\alpha$  (Fig. 1), so that

$$\cos \alpha = \cos \theta [1 + (V_\Omega / u_\infty)^2]^{-1/2}, \quad V_\Omega = \Omega R \sin \theta,$$

where  $\theta$  — polar angle of the spherical coordinate system,  $V_\Omega$  — circumferential velocity of the drop at the point of incidence,  $\Omega$  — angular velocity of rotation of the sphere.

Further, it is assumed in [3], that the liquid remaining after the impact spreads over the surface, and at the moment of the cessation of spreading, the shape of the liquid contact spot with the surface is an ellipse with semi-axes

$$a_l = r_l \cos^{-2/5} \alpha, \quad b_l = r_l \cos^{1/5} \alpha;$$

for the maximum radius  $r_l$  of the contact spot in normal collision ( $\alpha = 0$ ) an estimate was obtained:

$$r_l \sim \frac{2\xi^{5/12} a_d}{\sqrt{6}} \left( \frac{\rho_l v_n a_d}{\mu_l} \right)^{1/4}. \quad (1)$$

A classic example of a significant deformation in a force field is a drop hanging on a stream. In contrast to this situation, the solidification of a supercooled drop after collision with a rotating body is accompanied, in addition to elongation under the action of centrifugal force and possible disruption from its surface, by a complex of physical phenomena, in particular, nucleation, the velocity

of which depends on the characteristics of the shear flow of the liquid [6]; crystal growth, total volume which increases the effective viscosity of the suspension (for example, the well-known Einstein formula) and its thermal conductivity coefficient; by the release of phase transition heat, which is removed by heat exchange with flowing air and, possibly, radiation [7,8].

As the experiment [9] shows, a polar sharpening is formed even in case of a drop solidifying on a stationary substrate; needle-like icicles are formed in case of rotation of axisymmetric bodies (cone, ellipsoid), as already noted in Introduction [1,2].

The purpose of this work is to determine the shape and inclination of ice needles, as well as the place of their separation under the action of centrifugal force. The model proposed below is valid for drops of any size; of course, for small drops, the effects considered are not so expressive.

## 2. Physical and mathematical model

The abundance of complex physical processes leads to the need to build mathematical models using a number of simplifying assumptions and heuristic considerations. We will replace the liquid remaining on the surface with an equally large accompanying body of a simpler shape. The most suitable companion body for simulating the formation of a needle-shaped icicle is a cone. Unfortunately, the surface area of an inclined cone cannot be represented in elementary functions. Therefore, we will take a pyramid with a square base as a companion body. Note that the difference in the areas of contact with air for straight pyramids and cones of the same volume and height does not exceed  $\sim 10\%$ . One can hope that this is the same scale of error when replacing an unknown real shape of an ice needle with a conical one. This also allows considering the cone and the pyramid as equivalent figures and use both, based on the convenience of estimates.

Centrifugal force leads to elongation of the drop and a decrease in the area of its contact with the surface of a solid, reducing the energy of contact with air. In addition, the axis of the pyramid is tilted by angle  $\vartheta$  with respect to the local normal. The geometry of the accompanying pyramid is shown in Fig. 2.

Let's write down the change in the total surface energy due to the work of the centrifugal force

$$\begin{aligned} & \sigma_{la}(S_a - S_{a0}) + \sigma_{ls}(S_w - S_{w0}) - \sigma_{sa}(S_w - S_{w0}) \\ & = m\Omega^2 R(Y_c - Y_{c0})(\sin^2 \theta + \tan \vartheta_c \cos \theta \sin \theta). \end{aligned}$$

Here  $\sigma_{la}$ ,  $\sigma_{ls}$  and  $\sigma_{sa}$  — surface tension coefficients at the boundaries: liquid–air, liquid–solid, solid–air (indexes:  $l$  — liquid,  $a$  — air,  $s$  — solid). Then  $S_a$  and  $S_{a0}$  — the areas of the lateral surface (bordering the air) of the pyramid in the presence and absence of rotation,  $S_w$  and  $S_{w0}$  — corresponding the area of the base (in contact with the surface of the sphere — wall, index  $w$  — wall) of the

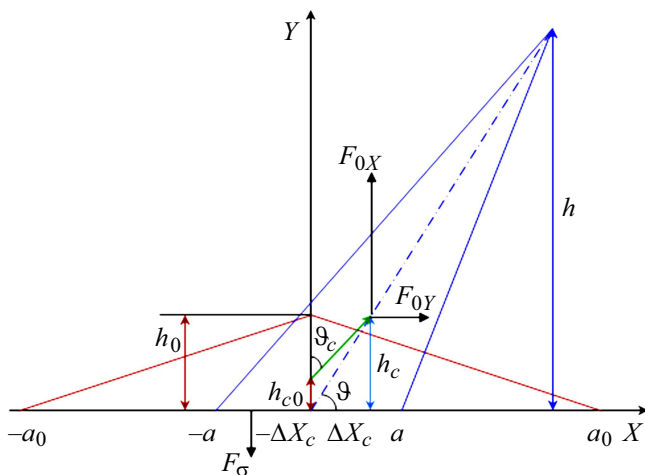


Figure 2. Geometry of the accompanying pyramid.

pyramid. Then  $Y_c$  and  $Y_{c0}$  — the corresponding coordinates of its center of mass in the perpendicular direction. Finally,  $\vartheta_c$  — the angle of inclination of the trajectory of the displacement of the center of mass, located at a distance of a quarter of the height of the pyramid. It is related to  $\vartheta$  by the ratio

$$\tan \vartheta = \tan \vartheta_c (1 - h_0/h).$$

where  $h_0$  and  $h$  — the height of the pyramid in the absence and in the presence of rotation. Thus, the first term describes the increment of the contact surface of a liquid with air, the second — with a solid, the third — of air with a solid. Further we will put  $\sigma_{la} \equiv \sigma$ . When writing the equation, the effect of gravity was neglected. In addition, it is taken into account that the main part of the cross-sectional area of the figure is in the boundary layer, so that the impact of aerodynamic force can be neglected. It is assumed that  $h \ll R$ , so that the centrifugal force can be considered constant on the scales of a drop or a companion body (pyramid).

With the dimensionless variables  $H = h/a$ ,  $H_0 = h_0/a_0$  ( $a$  and  $a_0$  — half the length of the side of the square of the base of the pyramid in the presence and absence of rotation) this equation has the form

$$\begin{aligned} & 2(1 + H^2)^{1/2} + [H^2 + (1 + H \tan \vartheta)^2]^{1/2} \\ & + [H^2 + (1 - H \tan \vartheta)^2]^{1/2} - 4(H/H_0)^{2/3}(1 + H_0^2)^{1/2} \\ & + 4 \cos \theta_\sigma [(H/H_0)^{2/3} - 1] = A\chi\xi^{2/3}H^{2/3}(H^{2/3} - H_0^{2/3}) \\ & \times (\sin^2 \theta + H^{2/3} \tan \vartheta \cos \theta \sin \theta), \end{aligned} \quad (2)$$

where  $\chi = 1/4$ ,  $A = 4\rho_l\pi^{2/3}a_d^2\Omega^2R/(3\sigma)$ .

Here we use the well-known relationship of three surface tension coefficients  $\sigma_{sa} = \sigma_{ls} + \sigma_{la} \cos \theta_\sigma$  ( $\theta_\sigma$  — wetting angle).

The equation (2) takes into account the conditions of conservation of volume  $V$  (and mass) of the drop remaining

on the surface of the rotating body:

$$V = 4\pi a_d^3 \xi / 3 = 4a^2 h / 3 = 4a_0^2 h_0 / 3.$$

The initial height of the pyramid is equal to

$$h_0 = \pi a_d^3 \xi / a_0^2.$$

The value  $a$  is related to the root of the equation (2) by the formula

$$a = a_d \sqrt[3]{\xi \pi / H}.$$

It is assumed that the front side of the square (the base of the pyramid) is perpendicular to the plane of the drop.

As the second physical condition, the equilibrium of the moments of forces relative to the point 0 — the center of the base of the pyramid of ice freezing to the body is assumed (Fig. 2):

$$F_{\Omega X} \Delta Y_c = (F_{\Omega Y} + F_\sigma) \Delta X_c.$$

Here  $F_{\Omega X}$ ,  $F_{\Omega Y}$  — the tangential and normal components of the centrifugal force,  $F_\sigma$  — the force of interaction of the particle with the surface,  $\Delta Y_c$  and  $\Delta X_c$  — displacements of the center of mass along the normal and tangent to the surface. It is assumed that due to the slope, the point of application of the force vector  $F_\sigma$  is shifted in the direction opposite to the slope, and its abscissa is  $-\Delta X_c$ . This displacement leads to a complex redistribution of stresses on the contact surface of the freezing drop and the substrate. The normal and tangential components of the resultant force of this interaction and its point of application are difficult to determine. The following considerations are used in this paper. First of all, the tangential component is of no interest, since it does not contribute to the balance of moments of forces relative to the center of the base of the pyramid. According to Young–Dupree law, the energy of this interaction is a value of the order of  $4a^2\sigma(1 + \cos \theta_\sigma)$ . An estimate of  $F_\sigma = a\sigma(1 + \cos \theta_\sigma)$  for the force is obtained attributing it to a contact line with a length of  $8a$ . As a result we have the following for determining the angle  $\vartheta$  of the slope of the pyramid axis with dimensionless variables:

$$\tan \vartheta = \frac{AH^{1/3} \cos \theta \sin \theta}{AH^{1/3} \sin^2 \theta + (1 + \cos \theta_\sigma)/2}. \quad (3)$$

It can be seen that at the angles  $\theta = 0$  and  $\pi/2$  (at the braking point and at the equator), there is no axis tilt, and at  $\theta_\sigma = \pi$  (absolute non-wettability), the force of interaction with the surface disappears (the second term in the denominator).

### 3. Numerical implementation and calculation results

Numerical studies have been carried out for the following set of defining parameters:  $u_\infty = 50$  m/s, drop radius  $a_d = 200 \mu\text{m}$ , sphere radius  $R = 15$  mm. With this set of

parameters, the motion of the drops can be considered rectilinear at a speed of  $V_d = u_\infty$ , since the Stokes number

$$\text{Stk} = \frac{2\rho_l a_d^2 u_\infty}{9\mu_a R} \approx 2 \cdot 10^4 \gg 1,$$

where  $\mu_a$  — air viscosity.

The following set of values of water and air parameters was assumed:  $\mu_a = 1.3 \cdot 10^{-5}$ ,  $\mu_l = 10^{-3}$  Pa · s;  $\rho_l = 10^3$  kg/m<sup>3</sup>;  $\sigma = 0.07$  N/m.

The initial value  $a_0$  was found when solving the equation (2) from the condition of equality of the contact areas of the drop and the accompanying pyramid

$$\pi a_l b_l = 4a_0^2,$$

which leads to the dependence of  $a_0$  on the drop fall angle  $\alpha$  and, consequently, the polar angle  $\theta$ :

$$a_0 = \frac{\sqrt{\pi} r_l}{2 \cos^{1/10} \alpha}.$$

The initial value  $H_0$  turns out to be quite small for the maximum radius  $r_l$  of the drop-to-surface contact spot determined by formula (1). So,  $H_0 \approx 0.02$  for the forward critical point ( $\theta = 0$ ). Solution of the equation (2) with such a  $H_0$  has a physical meaning (i.e.  $H = H_0$  with  $\theta = 0$ , where rotation is absent and increases with distance from the critical point) only in a narrow range of angle variation  $\theta_\sigma$  ( $0.9996 \leq \cos \theta_\sigma \leq 1$ ).

It needs to be reminded that the formula (1) was obtained in [3] under the assumption that the kinetic energy of the falling drop dissipates due to the viscous friction force when the drop spreads over the surface. Obviously, this process should also depend on the wetting angle. When evaluating the work of the friction force, a fitting multiplier equal to  $\sqrt{6}$  was used, which was found based on comparison with the results of [4] for small drops ( $a_d = 10 \mu\text{m}$ ).

In this paper, the value of  $H_0$  at the anterior critical point was changed with the change of adjustment multiplier and the critical value  $\theta_\sigma$  at which the solution of the equation (2) has a physical sense was determined. Obviously, the dependence  $H_0(\theta_\sigma)$  should be unambiguous and  $H_0(0) = 0$  (Fig. 3).

Fig. 4 shows the results of solving the equation (2) for different values of the wetting angle  $\theta_\sigma$  at rotation speed  $f = 100$  Hz. The curve 1 corresponds to  $\theta_\sigma = 21^\circ$ . At this value  $\theta_\sigma$ , the frozen drop is retained on the surface over the entire range of variation of the polar angle  $\theta$ . There is no solution of equation (2) for  $\theta_\sigma = 24$  and  $31.5^\circ$  (curves 2 and 3) if  $\theta$  exceeds some critical value, which corresponds to the separation of the frozen drop from the surface. The specified values  $\theta_\sigma$  do not refer to any specific material of the streamlined sphere.

Figure 5 shows the corresponding dependencies of the height of the pyramid on  $\theta$ . The maximum height of the pyramid is  $\sim 1$  mm, which justifies neglecting the effect of the aerodynamic force on it when deriving the formula (3),

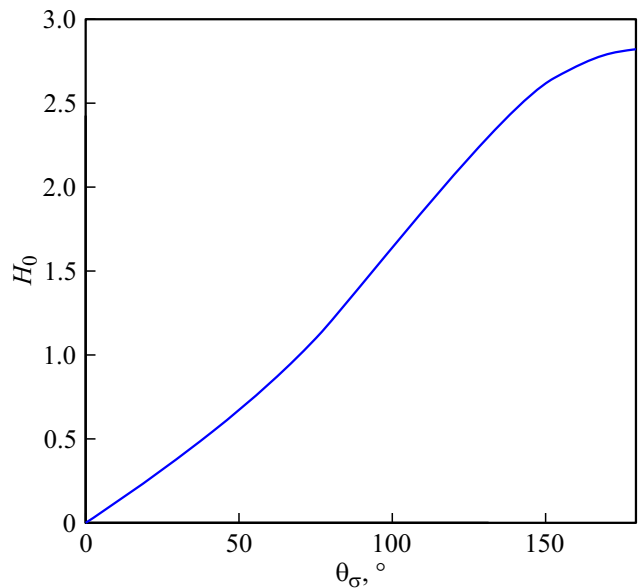


Figure 3. Dependence of the initial relative height of the pyramid at the point of flow deceleration on the wetting angle.

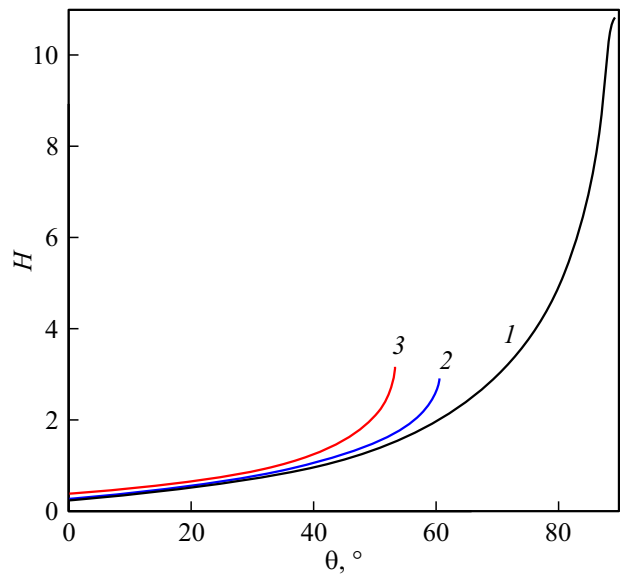
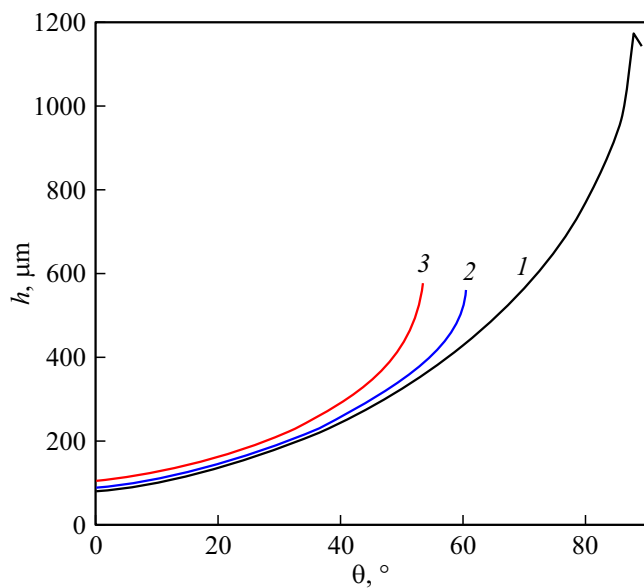


Figure 4. Dependence of the relative height of the hardened drop on the polar angle at the values of the wetting angle: 1 —  $\theta_\sigma = 21^\circ$ , 2 —  $24^\circ$ , 3 —  $31.5^\circ$ .

since the widest part of the pyramid is located in the boundary layer in which the air velocity tends to zero as it approaches the surface.

Finally, Figure 6 illustrates the non-monotonic dependence of the slope angle of the pyramid with respect to the local normal. It can be seen that the local angle of inclination increases with an increase of the polar angle (which determines the drop falling location) due to an increase of the centrifugal force perpendicular to the axis of rotation. It decreases after passing through the maximum,



**Figure 5.** Dependence of the height of the hardened drop on the polar angle at the values of the wetting angle: 1 —  $\theta_\sigma = 21^\circ$ , 2 —  $24^\circ$ , 3 —  $31.5^\circ$ .

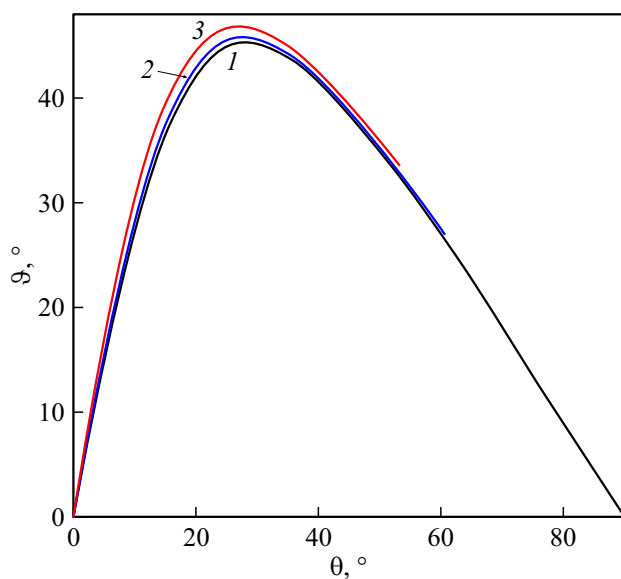


**Figure 6.** The dependence of the angle of inclination of the ice pyramid on the polar angle at the values of the wetting angle: 1 —  $\theta_\sigma = 21^\circ$ , 2 —  $24^\circ$ , 3 —  $31.5^\circ$ .

because in the direction of the equator, the local normal and the centrifugal force tend to combine.

## Conclusion

A model is proposed for calculating the geometric parameters of ice needles in the initial stage of ice formation on the surface of a rotating sphere, based on the use of the concept of an accompanying pyramid and a number

of simplifying assumptions, in particular, neglecting the impact of aerodynamic force and gravity. The results of the numerical study illustrate the main qualitative features of the phenomenon: the elongation of ice needles under the action of centrifugal force and their separation at certain values of angular velocity and polar angle on the surface of a rotating sphere, the non-monotonic dependence of the angle of inclination with respect to the local normal.

## Funding

The study was supported by the Russian Foundation for Basic Research, project 19-29-13024.

## Conflict of interest

The authors declare that they have no conflict of interest.

## References

- [1] L. Li, Y. Liu, H. Hu. *Exp. Therm. Fluid Sci.*, **109**, 109879 (2019). DOI: 10.1016/J.EXPTHERMFLUSCI.2019.109879
- [2] L. Tian, L. Li, Ha. Hu, Hu. *J. Thermophys. Heat Transf.*, **37** (2), 353 (2023). DOI: 10.2514/1.T6667
- [3] A.V. Kashevarov, A.L. Stasenko. *Tech. Phys.*, **65** (1), 41 (2020). DOI: 10.1134/S1063784220010120
- [4] P. Berthoumieu. *4th AIAA Atmospheric and Space Environments Conf.*, AIAA 2012–3130 (2012), DOI: 10.2514/6.2012-3130
- [5] R. Cimpeanu, D.T. Papageorgiou. *Intern. J. Multiphase Flow*, **107**, 192 (2018). DOI: 10.1016/j.ijmultiphaseflow.2018.06.011
- [6] A. Goswami, J.K. Singh. *Phys. Chem. Chem. Phys.*, **23** (29), 15402 (2021). DOI: 10.1039/D1CP02617H
- [7] M.E. Pereľman, V.A. Tatarchenko. *Phys. Lett. A*, **372** (14), 2480 (2008). DOI: 10.1016/j.physleta.2007.11.056
- [8] R. Stahlberg, H. Yoo, G. Pollack. *Indian J. Phys.*, **93**, 221 (2019). DOI: 10.1007/s12648-018-1265-6
- [9] L.B. Boinovich, A.M. Emelyanenko. *Dokl. Phys. Chem.*, **459** (2), 198 (2014). DOI: 10.1134/S0012501614120045

*Translated by Ego Translating*